

Dynamic quantitative photothermal monitoring of cell death of individual human red blood cells upon glucose depletion

Srivathsan Vasudevan
George Chung Kit Chen
Marta Andika

Nanyang Technological University
School of Electrical and Electronic Engineering
Photonics Research Center
50 Nanyang Avenue
Singapore 639798

Shuchi Agarwal
Peng Chen

Nanyang Technological University
School of Chemical and Biomedical Engineering
Division of Bioengineering
70 Nanyang Avenue
Singapore 637457

Malini Olivo

National Cancer Centre Singapore
Division of Medical Sciences
11 Hospital Drive
Singapore 169610
and

Biomedical Sciences Institutes
Singapore Bioimaging Consortium
11 Biopolis Way, #02-02 Helios
Singapore 138667
and

National University of Singapore
Department of Pharmacy
Blk S4, 18 Science Drive 4
Singapore 117543
and

National University Ireland
School of Physics
Galway, Ireland

1 Introduction

Human erythrocytes, or red blood cells (RBCs), have been found to undergo programmed cell death, or eryptosis, which could be caused by different triggers such as Ca^{2+} -ionophore,¹ oxidative stress,² energy depletion,³ etc. Eryptosis of RBCs is characterized by cell shrinkage, membrane blebbing, and the translocation of phosphatidylserine (PS) from the inner part of the plasma membrane to the external part of the cell.⁴ Since eryptosis is very similar to apoptosis of nucleated cells, analyzing it can lead to better understanding of the dynamics involved in the apoptosis process.⁵⁻⁹ Eryptosis can be triggered by a wide variety of diseases and by a large number of endogenous regulators,¹⁰ and hence this area has evinced considerable interest.

Abstract. Red blood cells (RBCs) have been found to undergo “programmed cell death,” or eryptosis, and understanding this process can provide more information about apoptosis of nucleated cells. Photothermal (PT) response, a label-free photothermal noninvasive technique, is proposed as a tool to monitor the cell death process of living human RBCs upon glucose depletion. Since the physiological status of the dying cells is highly sensitive to photothermal parameters (e.g., thermal diffusivity, absorption, etc.), we applied linear PT response to continuously monitor the death mechanism of RBC when depleted of glucose. The kinetics of the assay where the cell’s PT response transforms from linear to nonlinear regime is reported. In addition, quantitative monitoring was performed by extracting the relevant photothermal parameters from the PT response. Twofold increases in thermal diffusivity and size reduction were found in the linear PT response during cell death. Our results reveal that photothermal parameters change earlier than phosphatidylserine externalization (used for fluorescent studies), allowing us to detect the initial stage of eryptosis in a quantitative manner. Hence, the proposed tool, in addition to detection of eryptosis earlier than fluorescence, could also reveal physiological status of the cells through quantitative photothermal parameter extraction. © 2010 Society of Photo-Optical Instrumentation Engineers. [DOI: 10.1117/1.3484260]

Keywords: eryptosis; photothermal effects; cell death monitoring; linear response modeling and curve-fitting; thermal diffusivity.

Paper 10144R received Mar. 21, 2010; revised manuscript received Jun. 11, 2010; accepted for publication Jul. 6, 2010; published online Sep. 2, 2010.

Studies performed so far in eryptosis have investigated the different triggers that can either induce or inhibit eryptosis^{9,11} and the occurrence of eryptosis has been detected using flow cytometry. However, monitoring of the eryptosis process *per se* of individual RBCs has not been explored using any technique. Current techniques have only detected eryptosis but have not investigated the different physiological changes that occur within the cell during cell death except imaging the cells at different stages.¹ The cell death mechanism is a complex biochemical process that has several stages at different timings, and hence monitoring the kinetics of this process can provide very important information that can aid many clinical studies. For instance, during experiments on photodynamic therapy for selective killing of cancer cells, it is important to monitor the cell death process, as the dose of the inducing agent can lead the cell either to apoptosis or necrosis, two extremely different processes of cell death.¹² Thus, it is evi-

Address all correspondence to: George Chen, Nanyang Technological University, School of Electrical and Electronic Engineering, Photonics Research Center, 50 Nanyang Avenue, Singapore, Singapore 639798. Tel: 065-6790-4439; Fax: 065-6792-0415. E-mail: eckchen@pmail.ntu.edu.sg

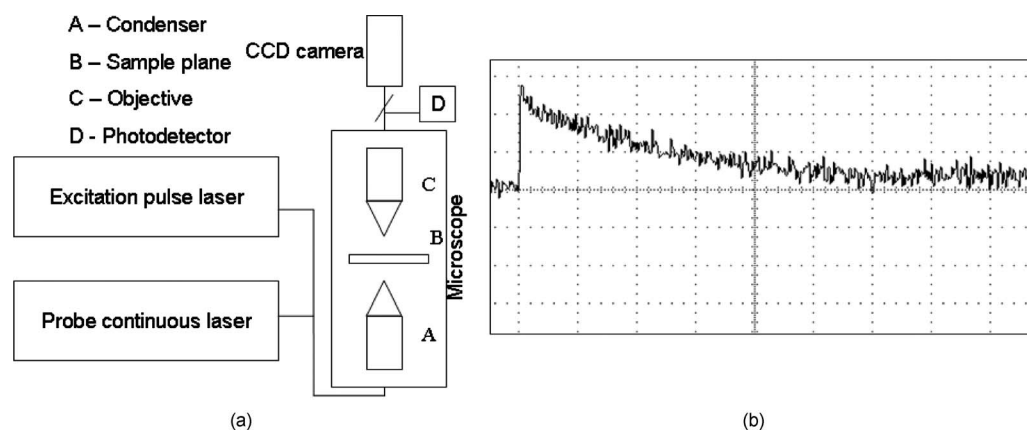


Fig. 1 (a) Experimental setup of PT response. (b) PT response of a healthy red blood cell, which consists of a fast rise time and a slow relaxation ($6 \mu\text{s}$) time (x axis, $2 \mu\text{s}/\text{div}$; y axis, $1.6 \text{ mV}/\text{div}$).

dent that monitoring the kinetics of eryptosis is significant, and it is more advantageous if the monitoring can be performed in a real-time, noninvasive manner. Continuously monitoring the biophysical changes of the cells during the eryptosis process without any exogenous markers can aid many clinical studies that are targeted toward early detection of diseases.¹⁰

Therefore, we propose to monitor the kinetics of the red blood cell death mechanism using a photothermal (PT) response technique, a noninvasive, marker-free technique that is suitable for real-time biomedical applications. PT response is a transient time-domain signal, consisting of a rise/drop and a relaxation time.^{13,14} As PT response is highly dependent on size, light absorption of cells, and thermal diffusivity of the target,¹⁵ the technique has been applied as a tool to monitor individual cells during many biomedical assays such as drug screening,¹⁶ nanoparticle photothermal tracking,¹⁷ etc.

Although PT response has been applied to many cellular level studies, these studies have merely utilized absorption as a parameter for detection.¹⁸ Besides absorption, other photothermal parameters such as thermal diffusivity, size, thermal interface contact resistance, etc. are also highly sensitive parameters that can reflect a cell's physiological status.¹⁹ For example, typical characteristics observed during eryptosis such as membrane blebbing, size shrinkage, etc. could alter certain photothermal parameters (e.g., size, thermal diffusivity) that are reflected in the PT response. However, these parameters have not been explored for cellular studies using PT response. In this paper, we report monitoring the effect of glucose depletion on human red blood cells (RBCs) by acquisition of PT response. The relaxation curve of the PT response, which reflects thermal diffusivity and size of the cell, is utilized as the principal feature of this study. Moreover, sufficiently low excitation energy was applied to the cells to obtain linear noninvasive PT responses. This allows reusability of the cells for further analysis. The investigation is further advanced by curve-fitting the PT response signal with our model, which has been developed to extract thermal diffusivity and size, thus providing a precise understanding of the parameter changes. Therefore, in addition to utilizing PT response as a monitoring tool, it can also aid to quantitatively analyze the bioassay (e.g., cell division, apoptosis) by extract-

ing the cell's photothermal parameters such as thermal diffusivity and size.

2 Materials and Methods

2.1 Photothermal Experiments

The pulsed excitation laser (Nd:YAG, 532 nm, 10 ns) and the continuous probe laser (He-Ne, 632.8 nm) are aligned to pass through a PT response microscope system that consists of a $10\times$ and $40\times$ microscope objective as condenser and imaging lenses, respectively, as shown in Fig. 1(a) (Ref. 20). The process begins with an excitation pulse irradiating on a target (e.g., cells). Light, absorbed by the targets, is converted to heat, thereby increasing the temperature of the targets and of the environment through diffusion. The increase in temperature induces a change in refractive index of the environment, thus producing a thermal lens that affects the focusing of the probe laser beam traversing through the heated region. The excitation pulse is filtered after transmitting through the microscope. The probe beam reaches the photodetector (Newfocus Photoreceiver, 125 MHz), which is connected to an oscilloscope (Hewlett Packard, 500 MHz) to obtain the PT response. PT response, a time domain signal, in general consists of a peak front due to the thermal lens formation and a relaxation tail due to subsequent heat diffusion. Rise time (time to reach the peak amplitude) and the amplitude of the PT response signal characterize the size and the absorption of the target, respectively. The relaxation time, τ_d (time duration for exponential decay from the peak intensity) is related to the size of the target and the thermal diffusivity. Figure 1(b) depicts the PT response signal of a healthy RBC, showing the different features of the response signal. A typical PT response consists of a sharp rise time and a slow relaxation time when the signal reverts to normal. This process would typically happen in the microseconds regime for cells. To acquire PT response, individual red blood cells were placed at the center of the excitation and probe laser beams of the PT response microscope system.

2.2 Modeling of PT Response

A mathematical model depicting the experimental situation is developed to curve-fit the experimental data and extract parameters such as thermal diffusivity and physical size of the cell. The PT response model is developed assuming that a single spherical target is placed in a homogenous medium. Unlike existing models in photothermal response, two different thermal diffusivities with one for the cell and one for the medium were implemented in the developed model. In addition, the Gaussian factor of the probe beam has been accounted for. The model is based on solving the heat diffusion equations. The heat conduction problem is modeled as a single homogenous spherical particle of radius a immersed in an infinite homogenous medium. When an excitation pulse heats up the target, the temperature profile of the target and its environment is altered. The temperature profile in the frequency domain, obtained by solving the two media heat diffusion equation, is given by²¹

$$\bar{T}_1^\delta(r,s) = \frac{\Phi\alpha}{K_1\gamma_1} \left[1 + \frac{aK_2 \sinh(\gamma_1^{1/2}r)}{rK_1 D} \right], \quad 0 \leq r < a, \quad (1)$$

$$\bar{T}_2^\delta(r,s) = \frac{\Phi\alpha}{K_1\gamma_1 r} \frac{a [\sinh(\gamma_1^{1/2}a) - a\gamma_1^{1/2} \cosh(\gamma_1^{1/2}a)]}{(1 + \gamma_2^{1/2}a)D} \times \exp[-\gamma_2(r-a)], \quad r > a, \quad (2)$$

where T_1 and T_2 are the temperature excursion profiles inside and outside the target, respectively. α is the absorption coefficient of the target, (cm^{-1}), Φ is the fluence, (J/cm^2), r is the point of temperature analysis, K_1 and K_2 ($\text{W}/\text{cm K}$) are the thermal conductivities inside and outside the cell, respectively, and D is given by

$$D = \frac{\sinh(\gamma_1^{1/2}a) - \gamma_1^{1/2}a \cosh(\gamma_1^{1/2}a)}{(1 + \gamma_2^{1/2}a)} \left(1 + \frac{K_2\gamma_2^{1/2}}{h} + \frac{K_2}{ha} \right) - \frac{K_2}{K_1} \sinh(\gamma_1^{1/2}a), \quad (3)$$

where $\gamma_1 = s/v_1$, $\gamma_2 = s/v_2$ in the frequency domain, with v_1 and v_2 as the thermal diffusivities of the cell and the medium, respectively.

The temperature profile creates a variation of the refractive index of the target and that of the medium, thus producing a thermal lens effect that affects the phase of the probe beam, as given by

$$\Delta\vartheta(x,y,t) = k \int_{-\infty}^{+\infty} \eta(x,y,z) T_i(x,y,z,t) dz, \quad (4)$$

where $\Delta\vartheta(x,y,t)$ is the phase shift induced due to the refractive index heterogeneity, $\eta(x,y,z) = (dn/dT)(x,y,z)$ is the refractive index gradient with respect to temperature, and k is the wave number. The power of the probe beam, after traversing through the heated region at the sample plane, is detected at the photoreceiver plane and is given by²¹

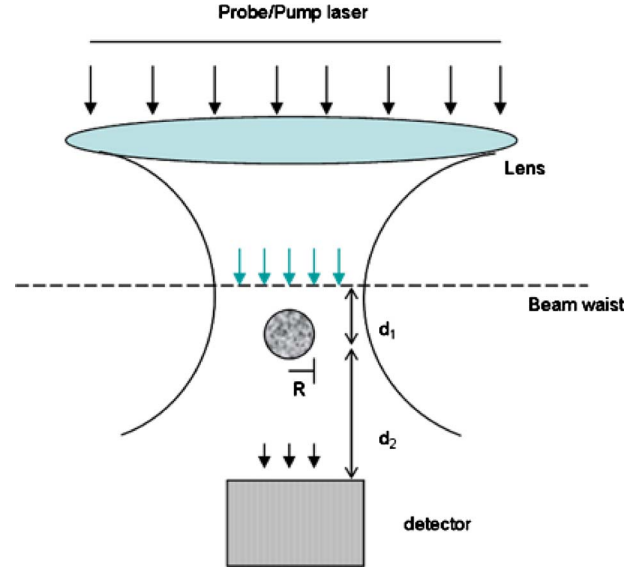


Fig. 2 Schematic diagram of PT response for theoretical model.

$$I(t) = 2\pi \int_{-R_0}^{R_0} \int_{-(R_0^2 - y^2)^{1/2}}^{(R_0^2 - y^2)^{1/2}} |U(x,y,d_1 + d_2,t)|^2 dx dy, \quad (5)$$

where d_1 is the distance between the target and the minimum waist of the probe beam, and d_2 is the distance between the target and the photoreceiver, respectively, as illustrated in Fig. 2. R_0 is the radius of the photoreceiver, and $U(x,y,d_1 + d_2,t)$ is the complex amplitude of the Gaussian probe beam at the photoreceiver plane and is given by

$$U(x,y,d_1 + d_2,t) = \frac{i}{\lambda(d_1 + d_2)w(d_1)} \left(\frac{2}{\pi} \right)^{1/2} \exp(-ikd_2) \times \left(\left\{ \exp \left[\frac{ik}{2q} (x^2 + y^2) \right] \exp[i\Delta\vartheta(x,y,t)] \right\} \right) ** \left\{ \exp \left[\frac{ik}{2(d_1 + d_2)} (x^2 + y^2) \right] \right\}, \quad (6)$$

where $**$ denotes convolution, q is the complex radius parameter of the Gaussian beam. The PTR signal can be calculated from the relative power change of the probe beam at the photoreceiver plane as

$$S(d_1 + d_2,t) = \frac{I(t) - I(\infty)}{I(\infty)}, \quad (7)$$

where $I(\infty)$ is the intensity when the time reaches infinity. For our model, $I(\infty)$ represents the intensity at 10 s, while the time domain PT response is in microseconds. Thus, the theoretical PT response is obtained from the developed model. Before being applied to cells, the same model was applied to PT responses of red polystyrene particles, and the results were found to be accurate. After this verification, the model was applied to curve-fit the experimental signal.

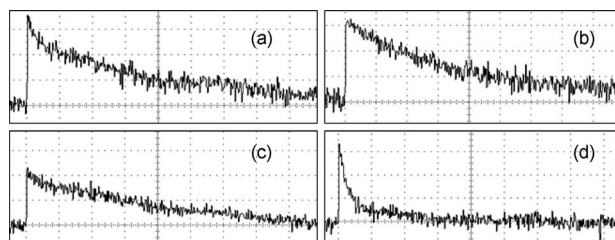


Fig. 3 PT response of RBC from (a) day 0 control (x axis, 2 $\mu\text{s}/\text{div}$; y axis, 800 $\mu\text{V}/\text{div}$); (b) day 0 test (x axis, 2 $\mu\text{s}/\text{div}$; y axis, 1 mV/div); (c) day 3 control (x axis, 2 $\mu\text{s}/\text{div}$; y axis, 1.6 mV/div); (d) day 3 test (x axis, 2 $\mu\text{s}/\text{div}$; y axis, 1.6 mV/div).

2.3 RBC Cell Preparation

Fresh human blood was obtained by venipuncture from healthy donors into 0.5% bovine serum albumin (BSA) solution in phosphate buffer saline (PBS) solution pH 7.4. Erythrocytes were then collected through centrifugation at 4 °C, 1000 G for 15 min. Experiments were performed with 0.3% hematocrit at 37 °C in Ringer solution (which contains 125 mM NaCl, 5 mM KCl, 1 mM MgSO₄, 32 mM HEPES, 5 mM glucose, 1 mM CaCl₂, pH 7.4).²² Glucose depletion solution was prepared by substituting glucose with 2.5 mM NaCl. All samples were incubated at 37 °C in a humidified atmosphere with 95% air and 5% CO₂.

Procured red blood cells were divided into two groups named control and test. The control group consisted of cells incubated with Ringer solution at 37 °C, and a constant pH was maintained.²³ The cells in the test group were incubated with Ringer solution depleted of glucose. As antioxidative defense requires energy, and that depends on glucose supply to red blood cells; the effect of glucose depletion induces cell death among red blood cells. RBCs while undergoing cell death process exhibit cell shrinkage, membrane blebbing, and microvesiculation.¹

2.4 Flow Cytometry Analysis

After incubation, erythrocytes were washed twice in annexin-binding buffer containing (in mM) 140 NaCl, 10 HEPES/NaOH, pH 7.4, and 5 CaCl₂ centrifuged at 200 G for 5 min and resuspended in 100 μl of Annexin-FLUOS labeling solution (1:100 dilution) (Roche Diagnostics GmbH, Mannheim, Germany) according to manufacturer’s protocol. The erythrocytes were incubated at room temperature for 15 min in the dark, followed by centrifugation and washing. Cells were analyzed by flow cytometry using a flow cytometer (BD FACS Calibur) at an excitation/emission of 488/518 nm.

3 Results

3.1 Red Blood Cell Assay

Glucose-depleted red blood cells were found to undergo eryptosis after 3 days of incubation, which has been reported in the literature. Hence, PT response was performed on the control and test groups (excitation energy, 0.25 μJ ; probe power, 1.5 mW) on day 0 as well as on day 3 after incubation. The aim here is to detect the cell death process using the PT response technique. Figure 3(a) shows a typical PT response of a control cell, which has a sharp rise and a relaxation time of 5.8 μs . Similarly, the PT response of a test group’s RBCs also has a typical relaxation time of 6 μs , as shown in Fig. 3(b). Thus, on day 0, both the test and control group cells behave similarly, as expected. However, after three days of incubation, the red blood cells in the test group were undergoing the death process, as they had been depleted of glucose.²² The PT response relaxation time of the control cell acquired on day 3 was 6 μs , as shown in Fig. 3(c), and this was consistent with day 0 results. In contrast, the test cell relaxed very fast, with $\tau_d = 1.2 \mu\text{s}$ [Fig. 3(d)], which is more than three times shorter as compared to the control group.

To check the repeatability of the results obtained, PT responses were acquired for a population of 30 cells from each group on day 0 as well as on day 3. Figure 4 shows the

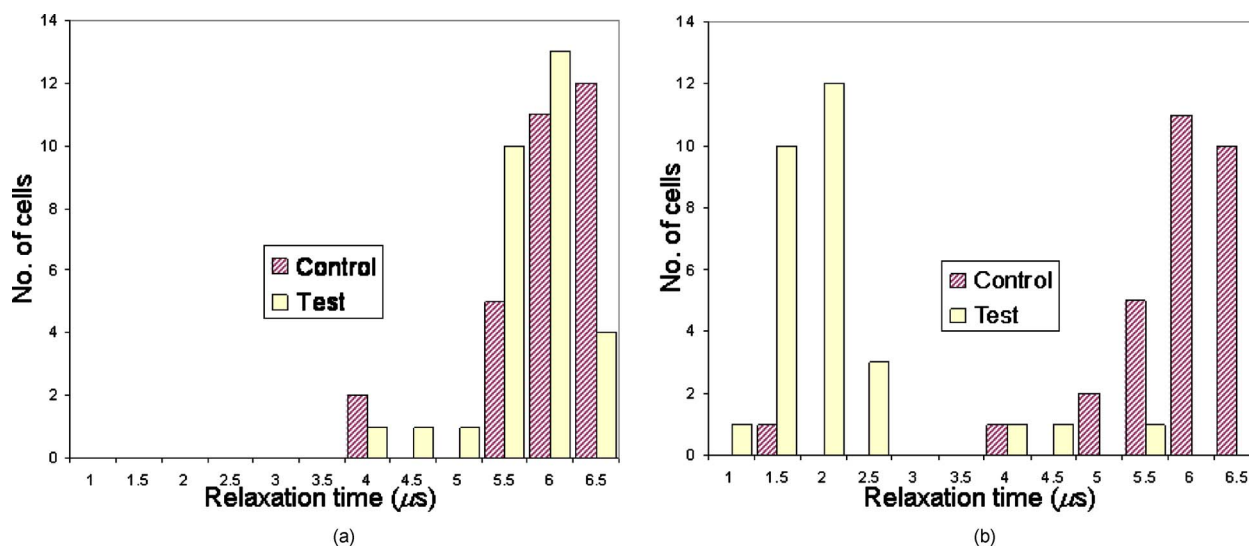


Fig. 4 Histogram of PT response relaxation curves of control and test groups on (a) day 0 and (b) day 3.

Table 1 Thermo-optical parameters of red blood cells.

Parameter	Value
Density (g cm ⁻³)	1.092
Specific heat (J/g·K)	3.77
dn/dT (C ⁻¹)	7 × 10 ⁻⁵
Refractive index	1.39
Absorption coefficient at 532 nm (cm ⁻¹)	135

histogram of the relaxation times of the population of cells during this assay. Figure 4(a) highlights that the relaxation times of both the control and test groups are very close, with average times of 6.15 μs and 5.9 μs, respectively, on day 0. In contrast, after three days of incubation, the average relaxation time of the test cell is 2.4 μs as compared to 6.06 μs of the control cell [Fig. 4(b)]. This illustrates that as the cells undergo eryptosis, relaxation time is shorter as compared to the control cells, thereby proving that the relaxation curve of the PT response can be used as a feature to monitor the cells in real time. An analysis of the photothermal parameters could delineate the reasoning behind the faster relaxation, as explained in the following section.

3.2 Extraction of PT Parameters from Experimental Results

The relaxation curve reflects two photothermal parameters—namely, thermal diffusivity and physical size. A faster relaxation curve of the dying cell could be due to either size shrinkage or increase in thermal diffusivity. Hence, extracting these two parameters from the PT response curve can give a clear picture of the biophysical changes of the dying cell.

Table 2 Extracted parameters from the curve-fitting process.

Parameter	Control cell	Test cell
Thermal diffusivity (cm ² /s)	0.0015	0.0029
Radius (μm)	2.52	2.12

The advantage of using PT response as a detecting tool is that the relevant photothermal parameters can be extracted. We applied our developed model to curve-fit the PT results obtained to extract thermal diffusivity and size of the cell from the control and test groups on day 3. The experimental results were normalized to avoid variations in the absorption of the PT response results. Equation (7) was used to curve-fit the experimental signals with the values $d_1=0.1 \mu\text{m}$ and $d_2=160 \text{ mm}$. The curve-fitting process was achieved by minimizing the error function:

$$E = \sum_{i=1}^N [f_m(i) - f_{ex}(i)]^2, \quad (8)$$

where $f_m(i)$ represents the data points of the theoretical model of the PT response, and $f_{ex}(i)$ shows the experimental data points with i representing the index of the data points. The values of other coefficients needed for the curve-fitting process are listed in Table 1. Figures 5(a) and 5(b) show the curve-fitted results of the control and test groups, respectively, and a least-squares optimization technique was used for the curve-fitting. The extracted thermal diffusivity and size are shown in Table 2. It is evident from the extracted values that the thermal diffusivity of the test cells increased by twofold, whereas the cell size decreased by 16%.

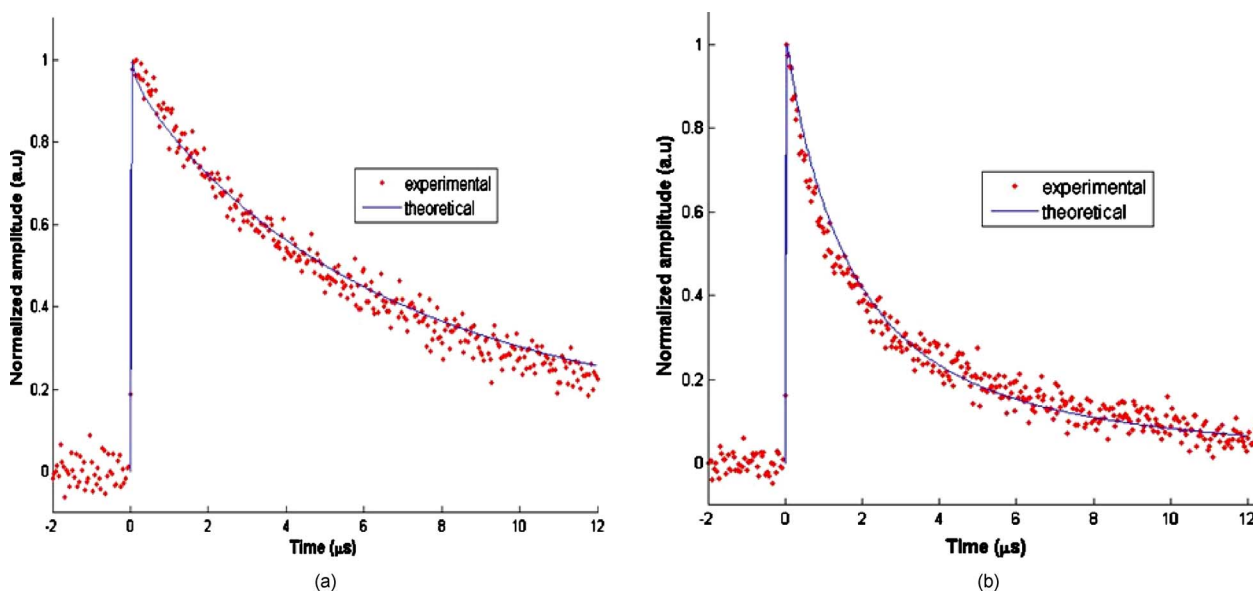


Fig. 5 Experimental and theoretical curve-fitted PT response results of (a) control cell and (b) test cell.

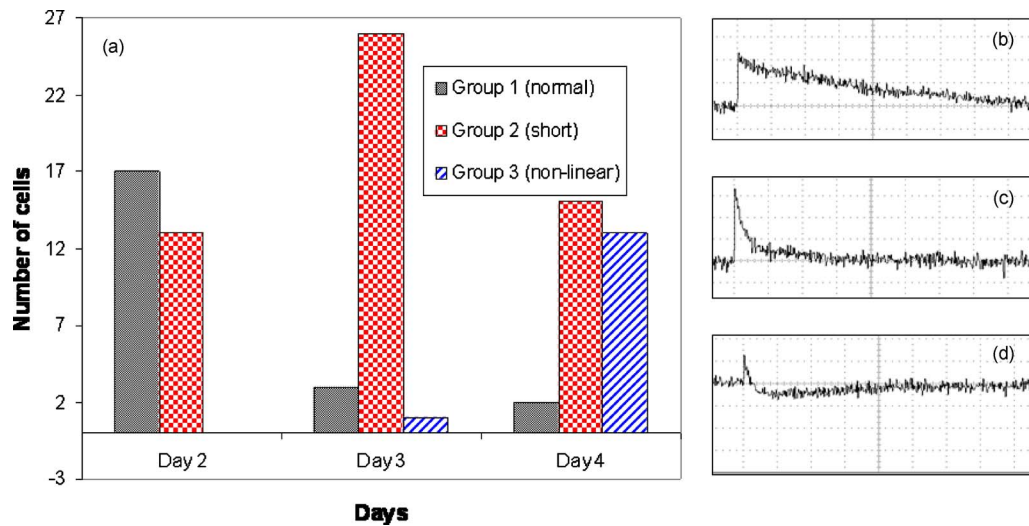


Fig. 6 (a) Monitoring the kinetics of the glucose depletion process of red blood cells. (b) Type 1 linear PT response (x axis, 2 μ s/div; y axis, 1.6 mV/div). (c) Type 2 linear PT response (x axis, 2 μ s/div; y axis, 1.6 mV/div). (d) Type 3 nonlinear PT response (x axis, 2 μ s/div; y axis, 2 mV/div).

3.3 Kinetics of RBC Eryptosis Experiment

The relaxation curve becomes shorter after three days of incubation for the test cells. It would be interesting to investigate the continuous change in the relaxation curve during the eryptosis process, as this would monitor the kinetics of the assay. This study is explored in this section. There was hardly any change in the PT response curve on day 1 compared to the control group, and hence the study was performed from days 2 to 4. While monitoring kinetics of the death process on days 2 to 4, three different types of PT responses were observed for the same excitation energy of 0.25 μ J and probe power of 1.5 mW. Type 1 represents a normal PT response with $\tau_d \sim 6 \mu$ s, as shown in Fig. 6(b), while type 2 has a short relaxation time ($\tau_d \sim 2.5 \mu$ s), as shown in Fig. 6(c). Type 3 is a nonlinear PT response, as shown in Fig. 6(d), that is invasive to the cells. The nonlinear response is an extreme case where the orientation of the signal changes from positive to negative.

Figure 6(a) highlights the results of the kinetics. Day 2 corresponds mainly to type 1 responses along with some type 2 responses. However, day 3 was highly dominated by type 2

responses along with a smaller percentage of type 1 and 3 responses. Analysis of day 4 shows that most of the cells exhibited type 2 and 3 responses as compared to type 1. From this study, it is clear that as time progresses, the PT response of red blood cells transforms from a normal response to a shorter one and then proceeds to a nonlinear response. It would be interesting to perform the same experiment on day 5. However, increase in the Brownian motion of the cells due to size shrinkage²⁰ prevented us from acquiring sufficient experimental results.

3.4 Flow Cytometry Detection of Eryptosis

Flow cytometry was performed concurrently with PT response experiments using the standard Annexin-V binding marker. This marker binds to PS that is translocated from the inner part of the plasma membrane to the external surface of the cell. This analysis indicates that glucose depletion induced a PS externalization, a feature that is common in eryptosis of RBCs. On day 2, 36.44% of the cells from the test group underwent eryptosis, as shown in Fig. 7(a). Subsequent in-

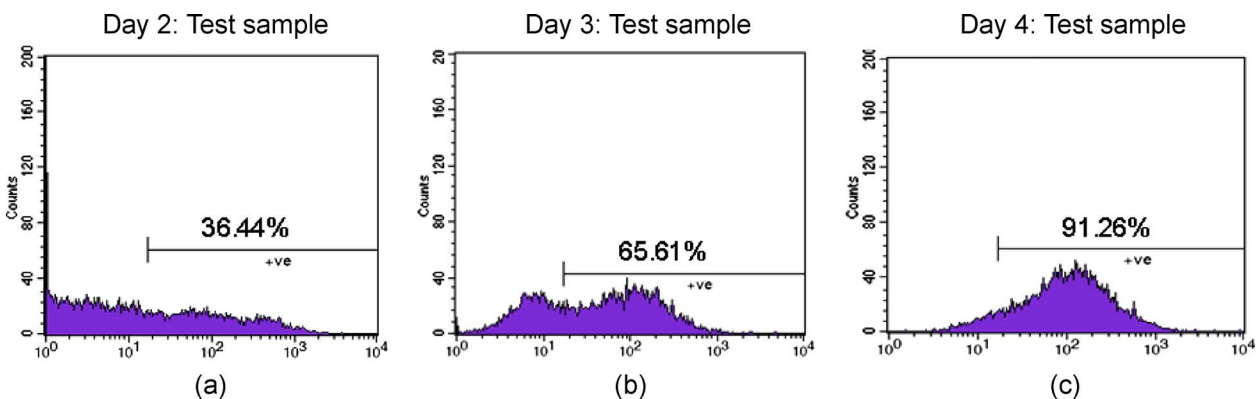


Fig. 7 Flow cytometry results of the test sample on three different incubation times.

Table 3 Comparison of PT response results with flow cytometry during RBC eryptosis of the test group.

Time point	PT response (%)	Flow cytometry (%)
Day 2	43.33	36.44
Day 3	90.00	65.61
Day 4	93.33	91.26

creases in eryptotic cells were observed on days 3 and 4 with 65.61% [Fig. 7(b)] and 91.26% [Fig. 7(c)], respectively, as shown in Table 3.

4 Discussion

In this paper, we proposed an efficient tool of detecting eryptosis using the relaxation time of the PT response. PT response was then utilized to continuously monitor the kinetics of the eryptosis process. It was found that as days progressed, the cells transformed from normal responses to shorter ones, before entering into a nonlinear regime. To confirm that the cells actually die, flow cytometry experiments were conducted concurrently, as shown in Fig. 7. Table 3 displays the percentage of cell death obtained from both PT response and flow cytometry of the test group cells. PT response percentage was calculated by counting the number of cells that exhibited types 2 and 3 responses. When analyzed with this criterion, it is evident from day 2 that PT response can detect cell death as accurately as flow cytometry. However, day 3 PT response results show a detection of 90% of eryptotic cells, which is much higher than that of flow cytometry (65.61%). But on day 4, both techniques once again detected a close percentage. To explain this seemingly strange result, we focus on the basic working principles of these two techniques. While flow cytometry works on the principles of detecting the Annexin-V fluorescence marker when it binds to PS that has been translocated to the outer cell membrane, the PT response detects the photothermal changes of the cells. Taking the PT response result as the same as the fluorescent result for day 3, as this is the case for both day 2 and day 4, the excessive 24% of the cells in type 2 and type 3 PT response suggests that there are some intracellular changes that significantly alter thermal properties (e.g., thermal diffusivity) of the eryptotic cells even before PS externalization. This is because photothermal properties of the cells continuously change during the eryptosis process, while the flow cytometry detects the PS externalization. Subsequently on day 4, when the PS is externalized for the 24% of the cells, the percentages of PT response and flow cytometry become close again. The analysis performed in this experiment is summarized in Table 4, where the different stages of the cell death process are correlated with photothermal parameter changes. Our finding suggests that there is an initial stage where thermal property change occurs before PS externalization, followed by a later stage where nonlinear response occurs after PS externalization.

It is evident that photothermal properties significantly reflect the cell's physiological status. To understand how these PT parameters change during the kinetics process, we applied

Table 4 Different stages of eryptosis compared to the photothermal parameter changes.

Stage	Characteristics	Regime
Initial	Thermal property changes with no PS externalization	Linear
Middle	Thermal property changes with PS externalization	Linear
Later	Substantial change in light absorption (optical property change)	Nonlinear

our model onto type 2 PT responses obtained from days 2 to 4 and extracted the PT parameters. Figure 8 highlights the results extracted from the curve-fitting process, which also compares the results to that of the control cells. The results, as shown in Fig. 8, clearly describe a drastic shrinkage in size from control to day 2, with a gradual decrease on the subsequent days. In addition, an increase in thermal diffusivity was observed as days progressed. Although these two photothermal parameters were independent during the curve-fitting process, it is known that these two parameters are actually related according to the following equation:

$$v_1 = \frac{K_1}{\rho_1 c_1}, \tag{9}$$

where ρ_1 is the density, and c_1 is the specific heat of the cell. Our curve-fitting results and previous report on red blood cell programmed cell death¹ confirm that the size of the cell starts to shrink first, before the membrane blebs. Shrinking of size should increase the density, assuming that there is no change in the mass of the cell. Thus, increase in density should decrease thermal diffusivity of the cell, assuming that other parameters in Eq. (9) remain constant. On the contrary, the curve-fitting results show that the thermal diffusivity actually increases. This indicates that thermal conductivity (K_1) should increase considerably to compensate for the drop caused by the density increase, as shown in Eq. (9). Increase

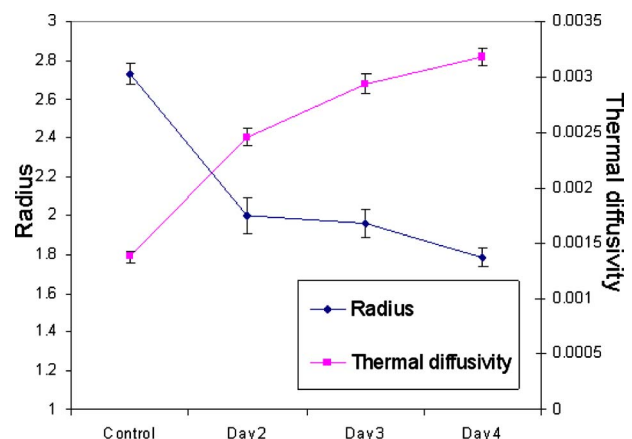


Fig. 8 Extracted photothermal parameters of RBCs from different days.

in K_1 is understandable according to the physics of materials, where increase in density can increase in thermal conductivity.²⁴ Similarly for a fluid with a greater density, its thermal conductivity could be higher as compared to a lower density fluid. It was confirmed from the microscopic images that the cell has shrunk during eryptosis, which increases the density. Hence, increase in density of the fluid could be a reason for the increase in the thermal conductivity.

As mentioned earlier, there is a transition from linear to nonlinear PT response of the dying cell as days progress. It is also evident from Fig. 8 that during the linear responses from day 0 to day 4, there is a continuous increase in thermal diffusivity. In addition to this, it is also seen that on day 4, more cells exhibited nonlinear PT responses as compared to type 1 and 2 responses. This could be because the excitation pulse, in addition to heating, could also cause bubble formation or intracellular component damage that could lead to a nonlinear type 3 response.²⁵ Since the same excitation energy was used on all days, bubble formation or intracellular component damage during the later stage is responsible for the substantial increase in type 3 responses on day 4. Thus, our results suggest that during the initial stages of eryptosis, there is a change in thermal property (i.e., thermal diffusivity), and at a later stage, the optical property of the cell (i.e., light absorption) is affected.

To understand the transformation of the PT response curve from linear to nonlinear, we explore the utilization of the absorbed energy after exciting the cell. Cellular structures absorb the excitation energy and can either diffuse the heat or utilize the energy for some chemical processes.²⁶ For example, oxidized molecules release the energy in terms of heat, while a reduced molecule may consume the heat for chemical processes, and thus a lesser amount of heat is diffused to the surrounding environment. Thus, a change in the redox state of the absorbing cellular structures may influence the PT response results. In our case, glucose depletion of RBCs reduces defense of the cell and hence induces oxidative stress.²³ Hemoglobin, present in RBCs, binds to oxygen reversibly, and oxidative stress may induce a change in the redox state of the hemoglobin.²⁷ Hence, a change in the redox state coupled with an increase in absorption may alter the cell chemically, which could either cause damage to the cell or trigger bubble formation, which leads to the formation of type 3 PT response. Therefore, our work emphasizes that the cells exhibited significant increase in thermal diffusivity at the initial stage and then increase in optical absorption at a later stage, which has been studied using the PT response.¹⁸ Thus, the proposed tool monitors the thermal property alterations quantitatively within the linear response and then detects the subsequent optical absorption change of the cells through the nonlinear response.

From the preceding discussion, we understand that photothermal parameters can be used to analyze many biological assays quantitatively. For example, analyzing how the photothermal parameters change during the apoptosis process can yield additional information about the death mechanism. Flow cytometry or fluorescent techniques can show only the percentage of dying cells using Annexin-V binding.²⁸ Hence, the fluorescent technique can only offer a way to detect cell death and cannot reveal the internal changes of the cells that occur during the cell death mechanism. In contrast, the PT response

is a pure physical monitoring tool, and this study shows that it has the ability to monitor an assay at different time points. Thus, the PT response technique can be used to monitor continuously, unlike the fluorescent technique, which needs different fluorescent markers for different time points. Since the PT response can be acquired during a real-time assay in an aqueous microscopic environment suitable for cells, the proposed quantitative monitoring tool can be applied in many cellular-level applications.

5 Conclusion

Photothermal response has been explored to detect cellular changes during eryptosis of red blood cells when depleted of glucose. Unlike other studies using PT response, our study has shown that for the same amount of excitation energy, changes in linear response were observed during the initial stages of cell death and nonlinear response exhibited subsequently. Increase in thermal diffusivity by twofold and size shrinkage were discovered from the linear PT response curves of the dying cells. The increase in thermal diffusivity suggests a considerable increase in thermal conductivity, which is attributed to a higher density of the cell. In the proposed tool, linear response monitors the thermal properties quantitatively, and subsequently nonlinear response reflects the optical absorption of cells.

Based on data analysis, it has also been inferred that the PT response can detect the initial stage of eryptosis before PS has been externalized. This is because the PT response monitors the changes in the thermal property of the cell, whereas flow cytometry detects only PS externalization. Therefore, the PT response can provide additional information above the initial stage of eryptosis in addition to detection of cell death. Also, the PT response curve can be used to correctly identify the physiological status of the cells. This feature can be potentially applied in monitoring assays that could reveal biophysical understanding of the cell during assays. For example, analyzing the photothermal parameter changes that occur during apoptosis can be of potential use in early detection of cancer.

Acknowledgments

The authors thank Dr. Balpreet Singh Ahluwalia and Bhuvaneshwari R. for fruitful discussions. This work is supported by the Singapore Bio-Imaging Consortium under Grant No. RP C-015/2007.

References

1. D. Bratosin, J. Estaquier, F. Petit, D. Arnoult, B. Quatannens, J. P. Tissier, C. Slomianny, C. Sartiaux, C. Alonso, J. J. Huart, J. Montreuil, and J. C. Ameisen, "Programmed cell death in mature erythrocytes: a model for investigating death effector pathways operating in the absence of mitochondria," *Cell Death Differ* **8**(12), 1143–1156 (2001).
2. C. Durantou, S. M. Huber, and F. Lang, "Oxidation induces a Cl-dependent cation conductance in human red blood cells," *J. Physiol.* **539**(3), 847–855 (2002).
3. K. Lang, B. Roll, S. Myssina, M. Schittenhelm, H. G. Scheel-Walter, L. Kanz, J. Fritz, F. Lang, S. Huber, and T. Wieder, "Enhanced erythrocyte apoptosis in sickle cell anemia, thalassemia and glucose-6-phosphate dehydrogenase deficiency," *Cell. Physiol. Biochem.* **12**(5–6), 365–372 (2002).
4. C. P. Berg, I. H. Engels, A. Rothbart, K. Lauber, A. Renz, S. F. Schlosser, K. Schulze-Osthoff, and S. Wesselborg, "Human mature

- red blood cells express caspase-3 and caspase-8, but are devoid of mitochondrial regulators of apoptosis," *Cell Death Differ* **8**(12), 1197–1206 (2001).
5. M. Föller, D. Bobbala, S. Koka, S. M. Huber, E. Gulbins, and F. Lang, "Suicide for survival—death of infected erythrocytes as a host mechanism to survive malaria," *Cell. Physiol. Biochem.* **24**(3–4), 133–140 (2009).
 6. M. Föller, M. Sopjani, H. P. Schlemmer, C. D. Claussen, and F. Lang, "Triggering of suicidal erythrocyte death by radiocontrast agents," *Eur. J. Clin. Invest* **39**(7), 576–583 (2009).
 7. J. P. Nicolay, G. Liebig, O. M. Niemoeller, S. Koka, M. Ghashghaieinia, T. Wieder, J. Haendeler, R. Busse, and F. Lang, "Inhibition of suicidal erythrocyte death by nitric oxide," *Pflug. Arch. Eur. J. Phys.* **456**(2), 293–305 (2008).
 8. F. Lang, E. Gulbins, H. Lerche, S. M. Huber, D. S. Kempe, and M. Föller, "Eryptosis, a window to systemic disease," *Cell. Physiol. Biochem.* **22**(5–6), 373–380 (2008).
 9. H. Mahmud, D. Mauro, S. M. Qadri, M. Föller, and F. Lang, "Triggering of suicidal erythrocyte death by Amphotericin B," *Cell. Physiol. Biochem.* **24**(3–4), 263–270 (2009).
 10. M. Föller, S. M. Huber, and F. Lang, "Erythrocyte programmed cell death," *IUBMB Life* **60**(10), 661–668 (2008).
 11. T. N. Tan, M. Föller, and F. Lang, "Tin triggers suicidal death of erythrocytes," *J. Appl. Toxicol.* **29**(1), 79–83 (2009).
 12. N. L. Oleinick, R. L. Morris, and I. Belichenko, "The role of apoptosis in response to photodynamic therapy: what, where, why, and how," *Photochem. Photobiol. Sci.* **1**(1), 1–21 (2002).
 13. Q. He, R. Vyas, and R. Gupta, "Photothermal lensing detection: theory and experiment," *Appl. Opt.* **36**(27), 7046–7058 (1997).
 14. K. Uchiyama, A. Hibara, H. Kimura, T. Sawada, and T. Kitamori, "Thermal lens microscope," *Jpn. J. Appl. Phys.* **39**, 5316–5322 (2000).
 15. D. Lapotko, "Pulsed photothermal heating of the media during bubble generation around gold nanoparticles," *Int. J. Heat Mass Transfer* **52**(5–6), 1540–1543 (2009).
 16. D. Lasne, G. A. Blab, F. De Giorgi, F. Ichas, B. Lounis, and L. Cognet, "Label-free optical imaging of mitochondria in live cells," *Opt. Express* **15**(21), 14184–14193 (2007).
 17. D. Lasne, G. A. Blab, S. Berciaud, M. Heine, L. Groc, D. Choquet, L. Cognet, and B. Lounis, "Single nanoparticle photothermal tracking (SNaPT) of 5-nm gold beads in live cells," *Biophys. J.* **91**(12), 4598–4604 (2006).
 18. V. P. Zharov, V. Galitovskiy, C. S. Lyle, and T. C. Chambers, "Superhigh-sensitivity photothermal monitoring of individual cell response to antitumor drug," *J. Biomed. Opt.* **11**(6), 064034 (2006).
 19. D. Lapotko, A. Shnip, and E. Lukianova, "Photothermal responses of individual cells," *J. Biomed. Opt.* **10**(1), 014006 (2005).
 20. S. Vasudevan, G. C. K. Chen, and B. S. Ahluwalia, "Integration of laser trapping for continuous and selective monitoring of photothermal response of a single microparticle," *Opt. Lett.* **33**(23), 2779–2781 (2008).
 21. M. Andika, G. C. K. Chen, and S. Vasudevan, "Excitation temporal pulse shape and probe beam size effect on pulsed photothermal lens of single particle," *J. Opt. Soc. Am. B* **27**(4), 796–805 (2010).
 22. K. S. Lang, C. Duranton, H. Poehlmann, S. Myssina, C. Bauer, F. Lang, T. Wieder, and S. M. Huber, "Cation channels trigger apoptotic death of erythrocytes," *Cell Death Differ* **10**(2), 249–256 (2003).
 23. K. S. Lang, P. A. Lang, C. Bauer, C. Duranton, T. Wieder, S. M. Huber, and F. Lang, "Mechanisms of suicidal erythrocyte death," *Cell. Physiol. Biochem.* **15**(5), 195–202 (2005).
 24. R. Srinivasan, A. A. Irudayaraj, P. Kuppusami, E. Mohandas, S. Kalainathan, and K. Ramachandran, "Photoacoustic studies on TiAlN nanostructured thin films," *Int. J. Mod. Phys. B* **21**(22), 3889–3900 (2007).
 25. V. P. Zharov, "Photothermal imaging of nanoparticles and cells," *IEEE J. Sel. Top. Quantum Electron.* **11**(4), 733–751 (2005).
 26. D. Lapotko, T. Romanovskaya, and E. Gordiyko, "Photothermal monitoring of redox state of respiratory chain in single live cells," *Photochem. Photobiol.* **75**(5), 519–526 (2002).
 27. E. L. P. Larsen, L. L. Randeberg, O. A. Gederaas, H. E. Krokan, D. R. Hjelle, and L. O. Svaasand, "In vitro study on methemoglobin formation in erythrocytes following hexyl-aminolevulinat induced photodynamic therapy," in *Progress in Biomedical Optics and Imaging*, *Proc. SPIE* **6427**, 642719 (2007).
 28. H. A. Andree, C. P. Reutelingsperger, R. Hauptmann, H. C. Hemker, W. T. Hermens, and G. M. Willems, "Binding of vascular anticoagulant alpha (VAC alpha) to planar phospholipid bilayers," *J. Biol. Chem.* **265**(9), 4923–4927 (1990).